Inorg. Chem. **2009**, *48*, 4354−4361

Inorganic Chemistry
Article

Syntheses and Vibrational Circular Dichroism Spectra of the Complete Series of [Ru((−)- or (+)-tfac)$_n$(acac)$_{3-n}$] ($n = 0 \sim 3$, tfac = 3-Trifluoroacetylcamphorato and acac = Acetylacetonato)

Hisako Sato,[†,‡] Yukie Mori,[§,||] Yutaka Fukuda,[§] and Akihiko Yamagishi*[,§]

Department of Earth and Planetary Science, Graduate School of Science, The University of Tokyo, 7-3-1 Hongo, Bunkyo-ku, Tokyo 113-0033, Japan, PRESTO, Japan Science and Technology Agency, Tokyo, Japan, and Department of Chemistry, Faculty of Science, Ochanomizu University, 2-1-1, Otsuka, Bunkyo-ku, Tokyo 112-8610, Japan

Received October 16, 2008

Twenty four kinds of Ru(III) complexes expressed by the formula of Δ- or Λ-[Ru((−)- or (+)-tfac)$_n$(acac)$_{3-n}$] ($n = 1$, 2, and 3, (−)- or (+)-tfac = (−)- or (+)-3-trifluoroacetylcamphorato and acac = acetylacetonato) were prepared in a pure diastereomeric form. The separation of these diastereomers was accomplished chromatographically by rational use of two antipodal chiral columns. The separated complexes were identified by means of mass spectra, ^{1}H NMR, electronic circular dichroism, and partly X-ray diffraction analyses. When a pair of Δ- and Λ-[Ru(acac)$_3$] ($n = 0$) was added to this group, they constituted the complete series of mixed ligand complexes including ligand chirality under the condition of no mixing of chiral ligands. The vibrational circular dichroism (VCD) spectra of their $CDCl_3$ solutions were recorded in the wavenumber region of 1000∼1800 cm^{-1}. The results provided a benchmark for systematically examining the effects of the stereochemical properties on VCD spectra such as the degree of ligand substitution, ΔΛ configurations, geometrical isomerism, and ligand chirality. As a result, the geometrical isomers of *trans*- or *cis*-[Ru((−)- or (+)-tfac)$_2$(acac)] and *mer*- or *fac*-[Ru((−)- or (+)-tfac)$_3$] were clearly differentiated by their VCD signals, which was hardly possible from their IR spectra alone.

Introduction

Vibrational circular dichroism (VCD) is the extension of electronic circular dichroism (ECD) into the infrared and near-infrared regions of the spectrum where vibrational transitions occur in the ground electronic state of a molecule.[1,2] The method measures the differential absorption of left versus right circularly polarized IR radiation by a molecular vibration transition. One of the advantages of VCD over ECD is the large amount of information concerning 3N-6 vibrations, where N is the number of atoms in the molecule. Accordingly the VCD method has been extensively applied for studying the conformation of a chiral organic molecule in a solution.[3−28]

* To whom correspondence is addressed: Phone and fax: +81-3-5978-5575; e-mail: yamagishi.akihiko@ocha.ac.jp.
† The University of Tokyo.
‡ Japan Science and Technology Agency.
§ Ochanomizu University.
|| Present Address: RIKEN, 2-1 Hirosawa, Wako, 351-0198, Japan.

(1) (a) Hilario, J.; Drapcho, D.; Curbelo, R.; Keiderling, T. A. *Appl. Spectrosc.* **2001**, *55*, 1435. (b) Nafie, L. A. *Appl. Spectrosc.* **2000**, *54*, 1634.
(2) (a) Cheeseman, J. R.; Frisch, M. J.; Devlin, F. J.; Stephens, P. J. *Chem. Phys. Lett.* **1996**, *252*, 211. (b) Stephens, P. J. *J. Phys. Chem.* **1985**, *89*, 748.
(3) Monde, K.; Taniguchi, T.; Miura, N.; Nishimura, S.-I. *J. Am. Chem. Soc.* **2004**, *126*, 9496. (b) Monde, K.; Miura, N.; Hashimoto, M.; Taniguchi, T.; Inabe, T. *J. Am. Chem. Soc.* **2006**, *128*, 6000. (c) Taniguchi, T.; Miura, N.; Nishimura, S.-I.; Monde, K. *Mol. Nutr. Food Res.* **2004**, *48*, 246.
(4) Aamouche, A.; Devlin, F. J.; Stephens, P. J. *J. Am. Chem. Soc.* **2000**, *122*, 2346.
(5) Longhi, G.; Gangemi, R.; Lebon, F.; Castiglioni, E.; Abbate, S.; Pultz, V. M.; Lightner, D. A. *J. Phys. Chem. A* **2004**, *108*, 5338.
(6) Stephens, P. J.; Devlin, F. J. *Chirality* **2000**, *12*, 172.
(7) Freedman, T. B.; Cao, X.; Dukor, R. K.; Nafie, L. A. *Chirality* **2003**, *15*, 743.
(8) Guo, C.; Shah, R. D.; Dukor, R. K.; Cao, X.; Freedman, T. B.; Nafie, L. A. *Anal. Chem.* **2004**, *76*, 6956.
(9) Malon, P.; Keiderling, T. A. *Appl. Spectrosc.* **1996**, *50*, 569.
(10) Bour, P.; Hennifer, M.; Wiesser, H. *J. Phys.Chem. A* **1998**, *102*, 102.
(11) Morita, H. E.; Kodama, T. S.; Tanaka, T. *Chirality* **2006**, *18*, 783.
(12) Longhi, G.; Abbate, S.; Gangemi, R.; Giorgio, E.; Rosini, C. *J. Phys. Chem. A.* **2006**, *110*, 4958.
(13) Debie, E.; Jaspers, L.; Bultinck, P.; Herrebout, W.; Veken, B. V. D. *Chem. Phys. Lett.* **2008**, *450*, 426.
(14) Izumu, H.; Ogata, A.; Nafie, L. A.; Dukor, R. D. *J. Org. Chem.* **2008**, *73*, 2367.

10.1021/ic801971p CCC: $40.75
Published on Web 04/24/2009

In these years, the application of the VCD method has been extended to the scope of metal complexes.[16−28] The conformation of a coordinated ligand in a solution is analyzed by comparing calculated and experimental spectra.[21] The fine structures in vibrational energy levels as well as the presence of the cooperative dynamics among ligands are revealed by this spectroscopic method. In the case of tris(acetylacetonato)metal(III) complexes,[28] for example, two closely located energy levels for the out-of-phase stretches of C−O bonds were assigned with no ambiguity, and the order of these energy levels was deduced to be opposite between the closed-shell and open-shell complexes. The results demonstrated the significant effects of the d-electron configuration of a central metal ion on vibration transition energy. Interestingly the same effect has been noted in the theoretical studies on the Raman optical activity of analogous metal complexes.[29]

Motivated by these works, the present work has studied the VCD spectra of a group of mixed ligand complexes. It was intended to see how the VCD spectra were affected by the fundamental coordination characters such as ΔΛ configuration, ligand chirality, and geometrical isomerism for a series of systematically varying metal complexes. This kind of information would be of crucial importance for the further application of the VCD method in this field. For these purposes, a mixed ligand Ru(III) complex with acetylacetonato (denoted by acac) and (−)- or (+)-3-(trifluoroacetyl)-camphorato (denoted by (−)- or (+)-tfac, respectively) was chosen. Although there are a number of VCD works reported on camphor-type compounds, no study has been reported on the coordination effect of these molecules.[4−13] Twenty four kinds of Ru(III) complexes represented by the formula,

Scheme 1. Structures of (−)- and (+)-3-(Trifluoroacetyl)-camphors: (a) (−)-tfacH; (b) (+)-tfacH

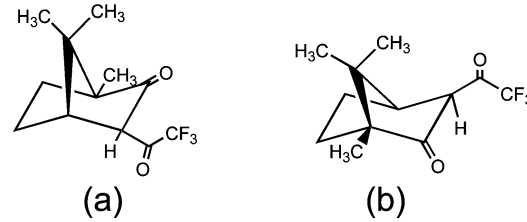

[Ru((−)- or (+)-tfac)$_n$(acac)$_{3-n}$] (n = 1, 2 and 3, tfac = 3-trifluoroacetylcamphorato and acac = acetylacetonato), were prepared and separated into pure diastereomers. The separation of these diastereomers was accomplished chromatographically by rational use of two antipodal chiral columns. The method has been developed in our own laboratory.[30] This is the first systematic study on the VCD spectra of a complete series of mixed ligand complexes under the limitation of no mixing of chiral ligand, each of which consists of homochiral ligands. Here both enantiomers of the tfac ligand, (−)-tfac and (+)-tfac, were used in order to prepare the antipodal pair of each diastereomer. The reliability of VCD spectra was confirmed by realizing the mirror image relation between antipodal pairs. The results are thought to provide a benchmark for developing a theoretical approach for the VCD spectra of open-shell molecules, since the investigated complexes contained a paramagnetic Ru(III) ion.

Results

Diastereomers of the Present Type of Mixed Ligand Complexes. Scheme 1 (a) and (b) show the structures of (−)- and (+)-3-(trifluoroacetyl)camphors (denoted by (−)-tfacH and (+)-tfacH), respectively. Scheme 2 (a)−(f) show the schematic drawings of possible mixed ligand complexes of [Ru((+)- or (−)-tfac)$_n$(acac)$_{3-n}$] (n = 1, 2, and 3). As shown in the scheme, the series contains 12 antipodal pairs of diastereomers, when the chirality of the ligands is taken into account.

Separation and Identification of Diastereomeric Isomers of [Ru((−)-tfac)$_n$(acac)$_{3-n}$] and [Ru((+)-tfac)$_n$(acac)$_{3-n}$] (n = 1, 2, and 3). A crude mixture of [Ru((−)-tfac)$_n$(acac)$_{3-n}$] (or [Ru((+)-tfac)$_n$(acac)$_{3-n}$]) (n = 1, 2, and 3) was obtained by the thermal reaction between [Ru(acac)$_3$] and (−)-tfacH (or (+)-tfacH). The separation into mono(tfac) (n = 1), bis(tfac) (n = 2) and tris(tfac) (n = 3) complexes was performed by eluting the crude product on a silica gel column with benzene (Experimental Section). The further separation of each fraction to individual diastereomers was performed by high performance liquid chromatography on a chiral column as below.

A mixture of mono(tfac) complexes ([Ru((−)-tfac)(acac)$_2$]) was eluted with methanol on a column packed with Δ-[Ru(phen)$_3$]$^{2+}$/synthetic hectorite.[30] Two peaks (denoted by **(−)-1P$_1$** and **(−)-1P$_2$**, respectively) were

(15) (a) Bieri, M.; Gautier, C.; Bürgi, T. *Phys. Chem. Chem. Phys.* **2007**, *9*, 671. (b) Gartier, C.; Bürgi, T. *J. Am. Chem. Soc.* **2006**, *128*, 11079.
(16) Barnet, C. J.; Drake, A. F.; Kuroda, R.; Mason, S. F.; Savage, S. *Chem. Phys. Lett.* **1980**, *70*, 8.
(17) (a) Morimoto, H.; Kinoshita, I.; Mori, M.; Kyogoku, Y.; Sugeta, H. *Chem. Lett.* **1989**, *18*, 73. (b) Teraoka, J.; Yamamoto, N.; Matsumoto, Y.; Kyogoku, Y.; Sugeta, H. *J. Am. Chem. Soc.* **1996**, *118*, 8875.
(18) (a) Young, D. A.; Lipp, E. D.; Daryl; Nafie, L. A. *J. Am. Chem. Soc.* **1985**, *107*, 6205. (b) Young, D. A.; Freedman, T. B.; Lipp, E. D.; Nafie, L. A. *J. Am. Chem. Soc.* **1986**, *108*, 7255. (c) Freedman, T. B.; Young, D. A.; Oboodi, M. R.; Nafie, L. A. *J. Am. Chem. Soc.* **1987**, *109*, 1551. (d) Young, D. A.; Freedman, T. B.; Nafie, L. A. *J. Am. Chem. Soc.* **1987**, *109*, 7674.
(19) He, Y.; Cao, X.; Nafie, L. A.; Freedman, T. B. *J. Am. Chem. Soc.* **2001**, *123*, 11320.
(20) (a) Freedman, T. B.; Cao, X.; Young, D. A.; Nafie, L. A. *J. Phys, Chem. A* **2002**, *106*, 3560. (b) Nafie, L. A. *J. Phys. Chem. A* **2004**, *108*, 7222.
(21) Lessen, P. R.; Guy, L.; Karame, I.; Roisnel, T.; Vanthuyne, N.; Roussel, C.; Cao, X.; Lombardi, R.; Crassous, J.; Feedman, T. B.; Nafie, L. A. *Inorg. Chem.* **2006**, *45*, 10230.
(22) Bas, D.; Bürgi, T.; Lacour, J.; Vachon, J.; Weber, J. *Chirality* **2005**, *17*, S143.
(23) Johannessen, C.; Thulstrup, P. W. *Dalton Trans.* **2007**, 1028.
(24) Amstrong, D. W.; Cotton, F. A.; Petrovic, A. G.; Polavarapu, P. L.; Warnke, M. M. *Inorg. Chem.* **2007**, *46*, 1535.
(25) Stephens, P. J.; Devlin, F. J.; Villani, C.; Gasparrini, F.; Mortera, S. L. *Inorg. Chim. Acta* **2008**, *361*, 987.
(26) (a) Nicu, V. P.; Neugebauer, J.; Baerends, E. J. *J. Phys. Chem. A* **2008**, *112*, 6978. (b) Nicu, V. P.; Autschbach, J.; Beaerends, E. J. *Phys. Chem. Chem. Phys.* **2009**, *11*, 1526.
(27) Taniguchi, T.; Monde, K.; Nishimura, S.-I.; Yoshida, J.; Sato, H.; Yamagishi, A. *Mol. Cryst. Liq. Cryst.* **2006**, *460*, 107.
(28) (a) Sato, H.; Taniguchi, K.; Nakahashi, A.; Monde, K.; Yamagishi, A. *Inorg. Chem.* **2007**, *46*, 6755. (b) Sato, H.; Taniguchi, T.; Monde, K.; Nishimura, S.-I.; Yamagishi, A. *Chem. Lett.* **2006**, *35*, 364.
(29) Luber, S.; Reiher, M. *Chem. Phys.* **2008**, *346*, 212.
(30) (a) Yamagishi, A. *J. Coord. Chem.* **1987**, *16*, 131. (b) He, J. X.; Sato, H.; Umemura, Y.; Yamagishi, A. *J. Phys. Chem. B* **2005**, *109*, 4679.

Scheme 2. Schematic Drawings of Possible Diastereomeric Isomers: A−B and C−C Represent (−)-tfac (or (+)-tfac) and acac, Respectively: (a) Mono(tfac) Complexes ([Ru((−)-or (+)-tfac)(acac)$_2$]), (b) *trans*-bis(tfac) Complexes (*trans*(I)-[Ru((−)- or or (+)-tfac)$_2$(acac)]), (c) *cis*-bis(tfac) Complexes (*cis*-[Ru((−)- or or (+)-tfac)$_2$(acac)]), (d) *trans*-bis(tfac) Complexes (*trans*(II)-[Ru((−)- or (+)-tfac)$_2$(acac)]), (e) *mer*-tris(tfac) Complexes (*mer*-[Ru-(−) or (+)-tfac)$_3$]), (f) *fac*-tris(tfac) Complexes (*fac*-[Ru((−)- or (+)-tfac)$_3$])

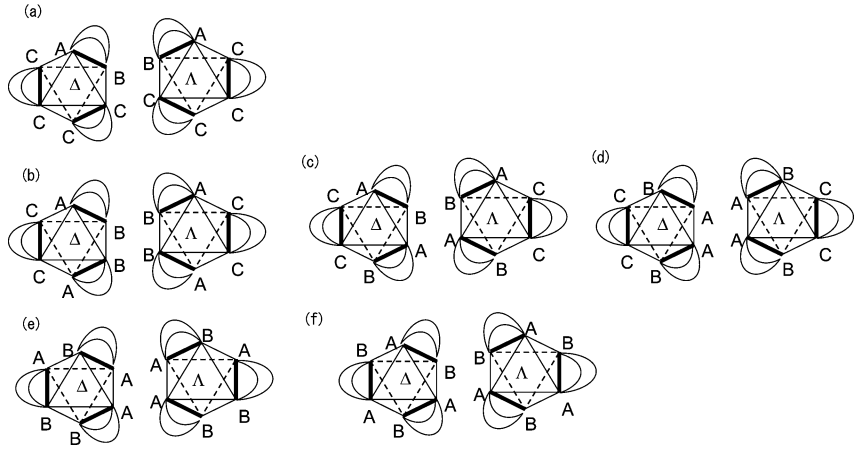

obtained on a baseline separation. By comparing the electronic circular dichroism (ECD) spectra of these fractions with those of Δ- or Λ-[Ru(acac)$_3$], **(−)-1P$_1$** and **(−)-1P$_2$** were identified to be Λ- and Δ-[Ru((−)-tfac)(acac)$_2$], respectively. ^{1}H NMR data were also consistent with these conclusions (Figures S1(a) and S3(a) and Table S1 (A) in the Supporting Information).

A mixture of bis(tfac) complexes ([Ru((−)-tfac)$_2$(acac)]) was eluted with methanol on the same column. Six peaks (denoted by **(−)-2P$_1$**, **(−)-2P$_2$**, **(−)-2P$_3$**, **(−)-2P$_4$**, **(−)-2P$_5$**, and **(−)-2P$_6$**, respectively) were obtained nearly on a baseline separation. From the ECD spectra of these fractions, **(−)-2P$_1$**, **(−)-2P$_2$**, and **(−)-2P$_4$** were identified to be Λ-isomers, whereas **(−)-2P$_3$**, **(−)-2P$_5$**, and **(−)-2P$_6$** were Δ-isomers. **(−)-2P$_1$**, **(−)-2P$_4$**, **(−)-2P$_5$**, and **(−)-2P$_6$** belonged to C_2 symmetry, or *trans* isomers, since two (−)-tfac ligands in these diastereomers were equivalent from their NMR spectra. The ECD spectra were similar between **(−)-2P$_1$** and **(−)-2P$_6$** or between **(−)-2P$_4$** and **(−)-2P$_5$**. Thus these corresponded to two different ΔΛ pairs of *trans*-[Ru((−)-tfac)$_2$(acac)]. They were denoted as *trans*(I)- and *trans*(II)-isomers, respectively. The structures of these two types of *trans*-isomers were differentiated with a help of X-ray diffraction analyses as described in the succeeding section. In the case of **(−)-2P$_2$** and **(−)-2P$_3$**, their NMR spectra indicated that two (−)-tfac ligands were unequivalent. Thus they were a ΔΛ pair of *cis*-[Ru((−)-tfac)$_2$(acac)] (Figures S1(b) and S3 and Table S1(B) in the Supporting Information).

A mixture of tris(tfac) complexes ([Ru((−)-tfac)$_3$]) was eluted with methanol on the same column. Four peaks (denoted by **(−)-3P$_1$**, **(−)-3P$_2$**, **(−)-3P$_3$** and **(−)-3P$_4$**, respectively) were obtained on a baseline separation. From the ECD spectra of these fractions, **(−)-3P$_1$** and **(−)-3P$_2$** were Λ-isomers, whereas **(−)-3P$_3$** and **(−)-3P$_4$** were Δ-isomers. In the case of **(−)-3P$_2$** and **(−)-3P$_3$**, their NMR spectra indicated that three (−)-tfac ligands were equivalent. Thus these diastereomers belonged to C_3 symmetry or were *fac*-isomers. No such symmetry was observed for **(−)-3P$_1$** and **(−)-3P$_4$**, indicating that they were *mer*-isomers. Based on these results, **(−)-3P$_2$** and **(−)-3P$_3$** were identified to be a ΔΛ pair of *fac*-[Ru((−)-tfac)$_3$], whereas **(−)-3P$_1$** and **(−)-3P$_4$** were a ΔΛ pair of *mer*-[Ru((−)-tfac)$_3$] (Figures S1(c) and S4 and Table S1(C) in the Supporting Information). The molar extinction coefficients of the UV−vis electronic absorption spectra were determined for the methanol solutions of the above diastereomeric metal complexes (Table S2 in the Supporting Information). The present HPLC separation might be compared with the previously reported method in which tris[(+)-3-acetylcamphorato]cobalt(III) complexes are separated to four diastereomers by means of thin-layer chromatography on silica gel.[31a]

For the other series of [Ru((+)-tfac)$_n$(acac)$_{3-n}$] (n = 1, 2, and 3) with opposite ligand chirality, chromatographic separation was performed on a column packed with Λ-[Ru(phen)$_3$]$^{2+}$/synthetic hectorite instead of Δ-[Ru(phen)$_3$]$^{2+}$/synthetic hectorite.[30] By using this column, the same diastereomeric relation was maintained between the adsorbent (column material) and the adsorbed molecules as in the case of [Ru((−)-tfac)$_n$(acac)$_{3-n}$] (n = 1, 2, and 3). As a result, on eluting a mixture of [Ru((+)-tfac)(acac)$_2$] with methanol, **(+)-1P$_1$**, and **(+)-1P$_2$** were obtained and identified to be Δ- and Λ-[Ru((+)-tfac)(acac)$_2$], respectively. For a mixture of [Ru((+)-tfac)$_2$(acac)], **(+)-2P$_1$**, **(+)-2P$_6$**, **(+)-2P$_2$** **(+)-2P$_3$**, **(+)-2P$_4$**, and **(+)-2P$_5$** were obtained and identified to be *trans*(I)-Δ- and *trans*(I)-Λ-[Ru((+)-tfac)$_2$(acac)], *cis*-Δ-[Ru((+)-tfac)$_2$(acac)] and *cis*-Λ-[Ru((+)-tfac)$_2$(acac)], *trans*(II)-Δ-[Ru((+)-tfac)$_2$(acac)], and *trans*(II)-Λ-[Ru((+)-tfac)$_2$(acac)], respectively. For a mixture of [Ru((+)-tfac)$_3$], **(+)-3P$_1$**, **(+)-3P$_4$**, **(+)-3P$_2$**, and **(+)-3P$_3$** were obtained and identified to be *mer*-Δ- and *mer*-Λ-[Ru((+)-tfac)$_3$], *fac*-Δ-[Ru((+)-tfac)$_3$], and *fac*-Λ-[Ru((+)-tfac)$_3$], respectively. In these ways, 24 kinds of Ru(III) complexes expressed by the formula, Δ- or Λ-[Ru((−)- or (+)-tfac)$_n$(acac)$_{3-n}$] (n =

(31) (a) Everett, G. W.; King, R. M., Jr. *Inorg. Chem.* **1972**, *11*, 2041. (b) Everett, G. W.; King, R. M. *Inorg. Chem.* **1971**, *10*, 1237.
(32) (a) Altomare, A.; Cascarano, G.; Giacovazzo, C.; Guagliardi, A.; Burla, M. C.; Polidori, G.; Camalli, M. *J. Appl. Crystallogr.* **1994**, *27*, 435. (b) Sheldrick, G. M. *SHELXL97, Program of the Refinement of Crystal Structures*; University of Gottingen: Germany, 1997.

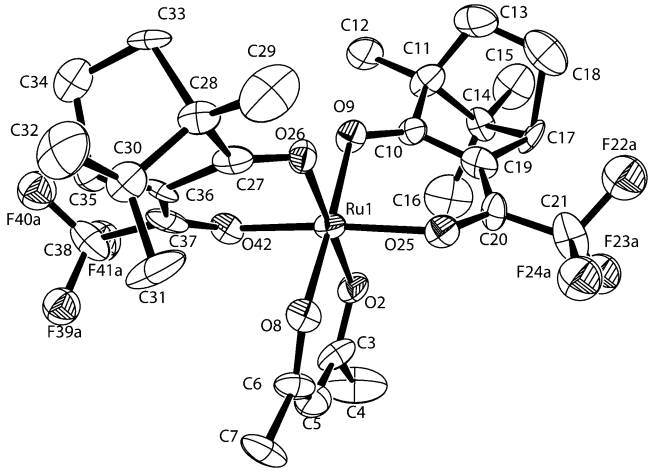

Figure 1. The ORTEP diagram of *trans*(I)-Λ-[Ru((−)-tfac)$_2$(acac)] with the thermal ellipsoids of 30% probability. The hydrogen atoms and one of the disordered CF_3 were excluded for clarity.

1∼3), were obtained in a pure diastereomeric form. They consisted of 12 antipodal pairs with opposite ΔΛ configuration and ligand chirality.

X-ray Crystallography of *trans*(I)-Δ-[Ru((−)-tfac)$_2$(acac)]. In the case of *trans*-[Ru((−)-tfac)$_2$(acac)], there were two possibilities as to the relative orientation of coordinated tfac ligands (Scheme 2 (b) and (d)). In accordance with these situations, two kinds of *trans*-[Ru((−)-tfac)$_2$(acac)] (denoted by *trans*(I)- and *trans*(II)-isomers) were obtained experimentally. X-ray crystallographic analyses were performed for *trans*(I)-Λ-[Ru((−)-tfac)$_2$(acac)]((−)-**2P$_1$**) to establish the structures of these isomers. Figure 1 shows the structure of one of the molecules. The selected bond distances and angles are listed in Supporting Information Table S3. Three bidentate ligands formed an octahedral coordination sphere of the ruthenium atom with the CF_3CO- groups located in the *trans*-relationship. The effect of the Jahn−Teller distortion on the electronic and vibrational properties was presumed to be small, since the variation of Ru−O bond distances was less than 6%. The bite angle of each ligand was close to 90° or slightly larger and each *trans*−O−Ru−O angle was close to 180°. The ruthenium atom was deviated by 0.23 Å from the O−C−C−C−O plane in the acac ligand, whereas the deviation distances for the (−)-tfac ligands were much larger (or 0.55 and 0.61 Å). In the crystals, some intermolecular interaction was suggested between H and F atoms because of the short distance (2.55 Å) between methyl and trifluoromethyl groups. Based on these results, it was established that *trans*(I)- and *trans*(II)-[Ru((−)-tfac)$_2$(acac)] isomers had two tfac ligands coordinated with their trifluoromethyl groups at *trans*- (Scheme 2 (b)) and *cis*-locations (Scheme 2 (d)), respectively.

Vibrational Circular Dichroism Spectra of Mixed Ligand Complexes. The VCD spectra of $CDCl_3$ solutions of the separated diastereomers were recorded in the wavenumber region of 1000∼1800 cm^{-1}. All of 12 pairs of optical antipodes gave mirror-imaged spectra over the whole wavenumber range, confirming the purity of diastereomers as well as the reliability of measurements.

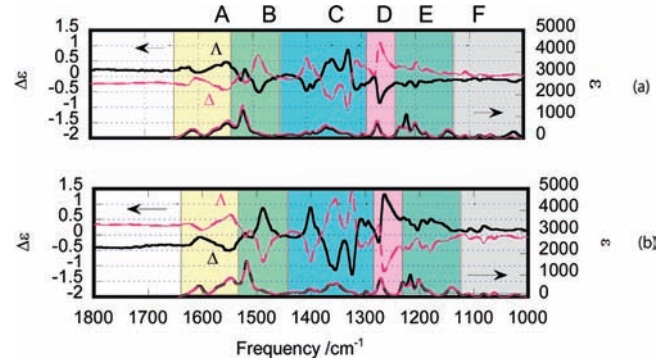

Figure 2. The observed VCD (upper) and IR (lower) spectra for two antipodal pairs of (a) Λ-[Ru((−)-tfac)(acac)$_2$)]/Δ-[Ru((+)-tfac)(acac)$_2$] and (b) Λ-[Ru((+)-tfac)(acac)$_2$]/Δ-[Ru((−)-tfac)(acac)$_2$)].

Figure 2 (a) and (b) show the observed VCD (upper) and IR (lower) spectra for two antipodal pairs of mono(tfac) complexes, Λ-[Ru((−)-tfac)(acac)$_2$]/Δ-[Ru((+)-tfac)(acac)$_2$] and Λ-[Ru((+)-tfac)-(acac)$_2$]/Δ-[Ru((−)-tfac)(acac)$_2$], respectively. The black and red lines corresponded to the complexes with (−)-tfac and (+)-tfac ligands, respectively. For characterizing the spectral features of these isomers, the spectra were divided into the following six regions: (Region A) the in-phase C−O stretches localized on either tfac or acac ligands (1650∼1550 cm^{-1}), (Region B) the asymmetric C−C−C stretching of diketonato parts of three ligands (1550∼1450 cm^{-1}), (Region C) mostly the out-of-phase C−O stretches of three ligands (1450∼1300 cm^{-1}), (Region D) the CH_2 wagging of a tfac ligand and the C−C−C in-plane bending of acac ligands (1300∼1250 cm^{-1}), (Region E) the CH_2 twisting and C−C−F asymmetric in-plane bending of a tfac ligand (1250∼1100 cm^{-1}),and (Region F) the CH_2 twisting, CH_2 wagging, symmetric CH_3 bending and C−C−H in-plane bending of a tfac ligand (1100∼1000 cm^{-1}). For comparison, the VCD results of the antipodal pairs of free ligands ((−)- or (−)-tfacH) and Λ-[Ru(acac)$_3$]/Δ-[Ru(acac)$_3$] are added in Figures S5 and S6 in the Supporting Information, respectively.

The spectra of mono(tfac) complexes ([Ru((−)- or (+)-tfac)(acac)$_2$]) were compared with those of enantiometic [Ru(acac)$_3$]. The additional band appeared at the highest wavenumber in region A in the IR and VCD spectra by replacing one acac ligand with one tfac ligand. Therefore the band was assigned to the C−O stretches intrinsic to the tfac ligands. In region C, three peaks were observed for [Ru(acac)$_3$] with alternatively changing signs, while one additional sharp peak appeared around 1320 cm^{-1} for [Ru((−)- or (+)-tfac)(acac)$_2$]. Thus this peak was assigned to the out-of-phase C−O stretches of the tfac ligand. These features on the effect of ligand substitution were more apparent in the VCD spectra than in the IR spectra.

Figure 3 (a)−(f) shows the observed VCD (upper) and IR (lower) spectra for six antipodal pairs of bis(tfac) complexes, Λ-*trans*(I)-[Ru((−)-tfac)$_2$(acac)]/Δ-*trans*(I)-[Ru((+)-tfac)$_2$(acac)], Λ-*trans*(I)-[Ru((+)-tfac)$_2$(acac)]/Δ-*trans*(I)-[Ru((−)-tfac)$_2$(acac)], Λ-*cis*-[Ru((−)-tfac)$_2$(acac)]/Δ-*cis*-[Ru((+)-tfac)$_2$(acac)], Λ-*cis*-[Ru((+)-tfac)$_2$(acac)]/Δ-*cis*-[Ru((−)-tfac)$_2$(acac)], Λ-*trans*(II)-[Ru((−)-tfac)$_2$(acac)]/Δ-*trans*(II)-[Ru((+)-tfac)$_2$(acac)], and Λ-*trans*(II)-[Ru((+)-tfac)$_2$(acac)]/Δ-*trans*(II)-[Ru((−)-tfac)$_2$(acac)], rspectively.

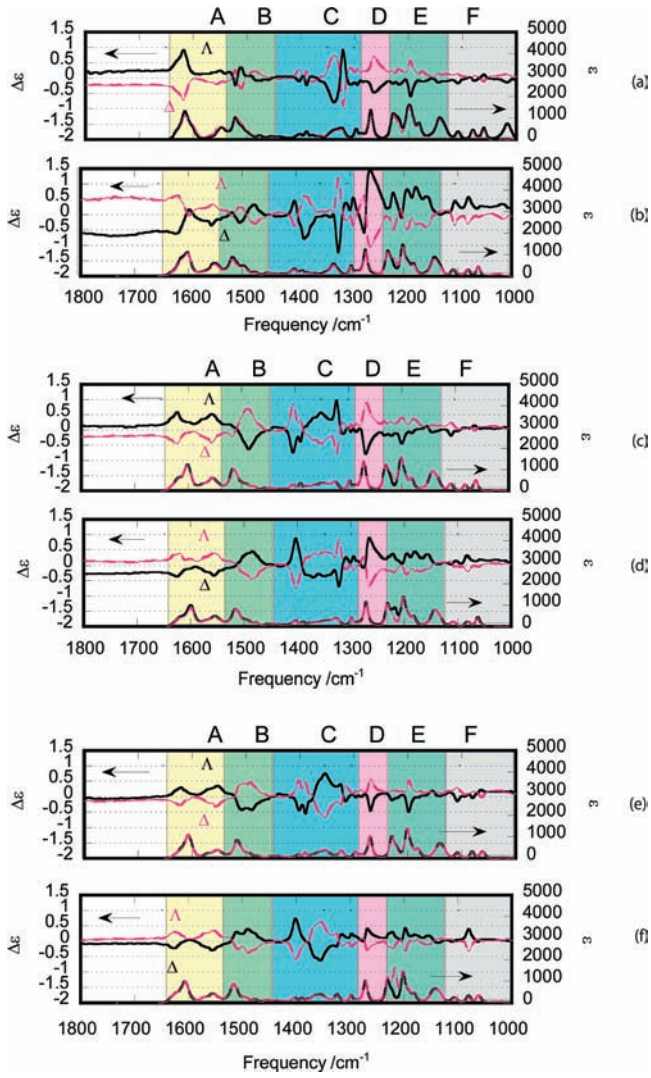

Figure 3. (a)−(f) The observed VCD (upper) and IR (lower) spectra for six antipodal pairs of (a) Λ-*trans*(I)-[Ru((−)-tfac)$_2$(acac)]/Δ-*trans*(I)-[Ru((+)-tfac)$_2$(acac)], (b) Λ-*trans*(I)-[Ru((+)-tfac)$_2$(acac)]/Δ-*trans*(I)-[Ru((−)-tfac)$_2$(acac)], (c) Λ-*cis*-[Ru((−)-tfac)$_2$(acac)]/Δ-*cis*-[Ru((+)-tfac)$_2$(acac)], (d) Λ-*cis*-[Ru((+)-tfac)$_2$(acac)]/Δ-*cis*-[Ru((−)-tfac)$_2$(acac)], (e) Λ-*trans*(II)-[Ru((−)-tfac)$_2$(acac)]/Δ-*trans*(II)-[Ru((+)-tfac)$_2$(acac)] and (f) Λ-*trans*(II)-[Ru((+)-tfac)$_2$(acac)]/Δ-*trans*(II)-[Ru((−)-tfac)$_2$(acac)].

The black and red lines indicate the complexes with (−)-tfac and (+)-tfac, respectively. For characterizing the spectral features of these isomers, the whole spectral region was divided into six regions in the same way as for the cases of mono(tfac) complexes.

One noteworthy aspect was the VCD spectra differed to a remarkable extent among the geometrical isomers, while there was little difference observed in the IR spectra. For example, in region A, *trans*(I)-isomers showed the strong and weak peaks at 1630 cm^{-1} and 1550 cm^{-1}, respectively, whereas *cis*- and *trans*(II)-isomers showed two peaks with equal intensity in the same region of the VCD spectra. These differential characters were absent in their IR spectra. As another aspect, the peak at the highest wavenumber (ca. 1400 cm^{-1}) in region C was split into two composites in the case of Λ-(−)- and Δ-(+)-complexes (Figure 3 (e)), while no such splitting was observed for the same peak in the case of Λ-(+)- and Δ-(−)-complexes (Figure 3 (f)). The effects could be related to the coupling of two different

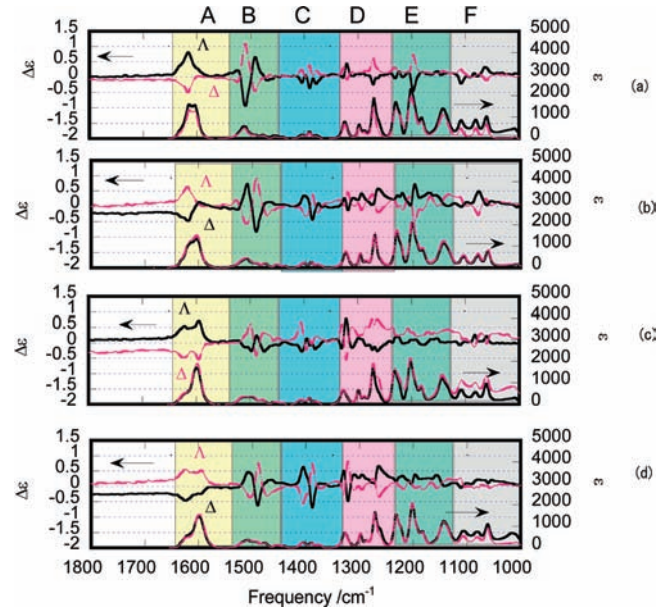

Figure 4. (a)−(d) The observed VCD (upper) and IR (lower) spectra for four antipodal pairs of (a) Λ-*mer*-[Ru((−)-tfac)$_3$]/Δ-*mer*-[Ru((+)-tfac)$_3$], (b) Λ-*mer*-[Ru((+)-tfac)$_3$]/Δ-*mer*-[Ru((−)-tfac)$_3$], (c) Λ-*fac*-[Ru((−)-tfac)$_3$]/Δ-*fac*-[Ru((+)-tfac)$_3$], and (d) Λ-*fac*-[Ru((+)-tfac)$_3$]/Δ-*fac*-[Ru((−)-tfac)$_3$.

chiralities, ΔΛ and RS, within one complex. The similar effect was also observed for mono(tfac) complexes (Figure 2 (a) and (b)).

Figure 4 (a)−(d) shows the observed VCD (upper) and IR (lower) spectra for four antipodal pairs of tris(tfac) complexes, Λ-*mer*-[Ru((−)-tfac)$_3$]/Δ-*mer*-[Ru((+)-tfac)$_3$], Λ-*mer*-[Ru((+)-tfac)$_3$]/Δ-*mer*-[Ru((−)-tfac)$_3$], Λ-*fac*-[Ru((−)-tfac)$_3$]/Δ-*fac*-[Ru((+)-tfac)$_3$], and Λ-*fac*-[Ru((+)-tfac)$_3$]/Δ-*fac*-[Ru((−)-tfac)$_3$], respectively. The black and red lines corresponded to the complexes with (−)-tfac and (+)-tfac ligands, respectively. For characterizing the spectral features of these isomers, the spectral region was divided into the following six parts: (Region A) the in-phase C—O stretches of tfac ligands (1650∼1550 cm^{-1}), (Region B) the asymmetric C—C—C stretching of diketonato parts of tfac ligands (1550∼1450 cm^{-1}), (Region C) mostly the out-of-phase C—O stretches of three ligands (1450∼1350 cm^{-1}), (Region D) the CH_2 wagging of tfac ligands (1350∼1250 cm^{-1}), (Region E) the CH_2 twisting and C—C—F asymmetric in-plane bending of tfac ligands (1250∼1100 cm^{-1}), and (Region F) the CH_2 twisting, CH_2 wagging, symmetric CH_3 bending and C—C—H in-plane bending of tfac ligands (1100∼1000 cm^{-1}).

All of four pairs gave similar IR spectra except for region A, in which the band consisted of two peaks with nearly equal intensity for the *mer*-isomers, while the same band consisted of one higher and one lower peaks for the *fac*-isomer. This difference was more prominent in the VCD spectra than in the IR spectra. Only one peak at the higher wavenumber was active for the *mer*-isomers, whereas both peaks were active with the same sign for the *fac*-isomers. Another notable aspect was that the chirality of ligands was less dominant than the ΔΛ configuration in determining the sign of the VCD peaks in most regions, whereas the situations were reversed in region F. The example was seen

for the middle peak among the three small peaks around 1080 cm^{-1} in region F. It was positive or negative for the complexes with (+)-tfac or (−)-tfac ligands, respectively, irrespective of the ΔΛ-configuration. No such tendency was observed for the mono(tfac) and bis(tfac) complexes. For them, the sign of all peaks was determined by the ΔΛ-configuration rather than by the ligand chirality. The results implied that the coupling among three ligands overcome the influence of the Δ or Λ configurations for the tris(tfac) complexes.

Discussion

This work has presented the first comprehensive VCD spectra for the *complete series* of tris(chelated) mixed ligand complexes, Δ- or Λ-[Ru((−)- or (+)-tfac)$_n$(acac)$_{3-n}$] (n = 0∼3), under the condition of no mixing of chiral enantiomeric ligands. As was previously pointed out, the present type of β-diketonato ruthenium(III) complexes exhibited remarkably high $\Delta\epsilon$-values (0.1∼1) in their VCD spectra.[28] These situations enabled us to compile each spectral data within a relatively short time (ca. 10 min). In spite of such short accumulation time, the mirror image relation observed for all of 13 antipodal pairs guaranteed the reliability of the measured spectra. The results are discussed from the viewpoint of how the stereochemical characters of the present type of complexes are manifested in their VCD spectra.

Enhancement of VCD Intensity of Chiral Ligands on Coordination. The spectra of metal complexes were compared with those of free ligands to see the effect of coordination on VCD activity. For that purpose, the IR and VCD spectra of $CDCl_3$ solutions of (−)-tfacH and (+)-tfacH were measured independently (Supporting Information Figure S5). As shown in the figure, the clear peaks were observed in the wavenumber region below 1100 cm^{-1}, which corresponded to the CH_2 twisting, CH_2 wagging, symmetric CH_3 bending and C—C—H in-plane bending of tfac ligands (region F). Thus the vibration peaks related to the asymmetric carbons were VCD-active whether the ligands were free or coordinated. To this contrary, no VCD peak was observed around 1700 cm^{-1} due to the C—O stretches for free ligands. This region corresponded to region A for the metal complexes, where the strong VCD peaks appeared due to C—O stretches. The results indicated that the C—O stretches remote from the asymmetric carbons in a free ligand (Scheme 1) became VCD-active under the helical coordination of the same ligands. It is suggested very recently that the enhancement of VCD intensities takes place due to the donor−acceptor interaction between the Cl^- base and N—H σ^* acceptor orbitals in the complexation of Cl^- counterions to $[Co(en)_3]^{3+}$.[26b] In the present complexes, the similar effect might operate in the interaction of d-electron orbitals in Ru(III) with tfac ligands.

Effects of Geometrical Isomerism. The present results enabled us to compare the VCD spectra among the geometrical isomers for bis(tfac) and tris(tfac) complexes. The difference among the geometrical isomers was manifested most remarkably in region A (in-phase stretches of C—O). In the case of bis(tfac) complexes, for example, two types of *trans*-isomers gave completely different spectral features; the *trans*(I)-isomer showed a single peak at higher wavenumber, whereas the *trans*(II)-isomer showed two peaks with equal intensity. It should be noted that both isomers exhibited nearly identical band shapes in their IR spectra. Thus such characterization was only possible with a help of VCD spectra. In the case of the tris(tfac) complexes, two peaks in regions A had different intensity, depending on the *mer*- or *fac*-isomers. In contrast to the bis(tfac) complexes cases, the IR spectra gave different spectral shapes for the geometrical isomers.

Effects of Ligand Chirality. The VCD spectra were compared between the diastereomeric pairs of Λ-[Ru((−)-tfac)$_n$(acac)$_{3-n}$]/Λ-[Ru((+)-tfac)$_n$(acac)$_{3-n}$] and Δ-[Ru((−)-tfac)$_n$(acac)$_{3-n}$]/Δ-[Ru((+)-tfac)$_n$(acac)$_{3-n}$] (n = 1 and 2). They had the same configuration with opposite ligand chirality. It was deduced that the signs of peaks were mostly dependent on the ΔΛ configuration, being little affected by the ligand chirality. The sign of the peaks intrinsic to the ligand chirality was also determined by the ΔΛ-configuration of a Ru(III) complex rather than the ligand chirality. These situations were seen for the peak around 1080 cm^{-1}, which was assigned to the bending of tfac ligands. For the free ligand, the peak was positive or negative for (+)- or (−)-tfacH, respectively, while its sign was dependent on the ΔΛ configuration in the case of the mono(tfac) and bis(tfac) complexes. The results might reflect the situations that these vibrations were not localized on a single tfac ligand in the bis(fac) complexes, but coupled with other two tfac ligands under the helically coordinating configuration. In fact, the theoretical calculation on mono(tfac) and bis(tfac) complexes showed that more than two ligands were involved simultaneously in the vibrational motions corresponding to the peaks in region F (Figure S10(a) and (b) in the Supporting Information). The situations differed a little in the case of tris(tfac) complexes. The sign of the middle peak at 1080 cm^{-1} in region F was determined by the ligand chirality irrespective of the ΔΛ-configuration. Thus the ligand chirality was a more predominant factor than the ΔΛ-configuration when the coupled three ligands were all of the same chirality. These results indicated that no simple additivity rule was maintained even for the vibrations intrinsic to tfac lignads.

Comparison with the Theoretical Prediction. There is a general belief that the magnetic field perturbation (MFP) theory for VCD is less applicable for the open-shell systems with the Jahn−Teller distortion.[2] In spite of this prevailing view, the theory predicted correctly the VCD spectra of Λ- and Δ-[Ru(acac)$_3$] in the previous works.[28] The situations that the Jahn−Teller distortion effects are so small in the present metal complexes as shown in Figure 2−4 motivated us to perform the calculations of the IR and VCD spectra on the basis of the same theoretical background.

One example for Δ-*fac*-[Ru((−)-tfac)$_3$] (**(−)-3P$_3$**) is shown in Figure 5. The details of calculations are given in the Experimental Section. When the figure is compared with the experimental observation (black solid line in Figure 4(d)), it is deduced that both the IR and VCD spectra are well reproduced by the present theory. The reasonable agreement

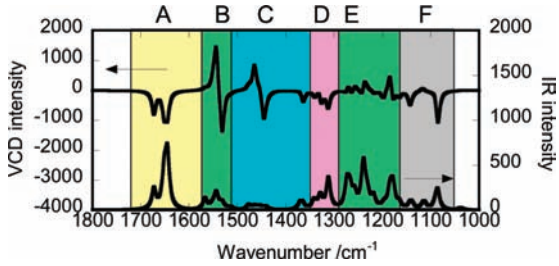

Figure 5. DFT-calculated VCD (upper) and IR (lower) spectra of Δ-*fac*-[Ru((−)-tfac)$_3$].

was seen for the spectra shapes in regions A, B, C, E, and F. Only exception was seen for region D in which the signoidal peaks around 1320 cm^{-1} and the broad positive peak around 1250 cm^{-1} in the VCD spectra were not in accord with the calculated spectra. Since the IR spectrum in this region was well predicted by the theory, it was speculated that these VCD peaks might arise from the low-lying excited states of the d-electrons in Ru(III). Apart from this disagreement, the assignment of the peaks in each region as described in the Results Section was validated by examining the vibrational motion for the calculated IR spectra.

The calculated results for mono(tfac), bis(tfac), and other tris(tfac) complexes are shown in Supporting Information Figures S8−S10. In the case of mono(tfac) complexes, the theory predicted well the sign of two peaks in region A, a peak in region B and the general feature of the band in region C. Notably it was predicted that the first peak in region C was doubly split for the Δ-(+)- (or Λ-(−)-) complexes, while no such split took place for the Λ-(+)- (or Λ-(−)-) complexes. In the case of bis(tfac) complexes, the theory succeeded in predicting the spectral feature of the band in region A. That is, the C−O band in region A was single for the *trans* (I)-isomer, while the same band consisted of two peaks for the *cis*- and *trans*(II)-isomers. As another aspect, the first band in region C was very weak for the *trans*(I)-isomer, whereas the same band was strong for the *cis*- and *trans*(II)-isomers. These features were predicted correctly by the theory. In the case of the tris(tfac) complexes as shown in Supporting Information Figure S9, the calculated IR and VCD spectra well reproduces the observed spectra in regions A and B except for the shift of each peak position toward higher frequency (ca. 70 cm^{-1}). For example, the geometrical isomerism on VCD spectra was predicted correctly by the theory. That is, the peak at lower wavenumber for the C−O band in region A was very low in VCD spectra for the *mer*-isomer, while the same peak has nearly equal intensity to the peak at higher wavelength for the *fac*-isomers. The theory might owe its successful prediction partially to the situations that the Jahn−Teller distortion from the octahedral structure was negligibly small in the present complexes.

Vibrational Details As Revealed by VCD Measurements. The VCD spectra may provide the information on the vibrational properties of a molecule that is not obtained by the IR spectra alone. In region C corresponding to the bands due to the C−O stretches of the present complexes, for example, the IR spectra gave a broadband with two or three maxima. In contrast, the fine-structures of the same band were clearly seen in the VCD spectra. When the VCD spectra were compared between Δ- or Λ-[Ru(acac)$_3$] and Δ- or Λ-[Ru((−)-tfac or (+)-tfac)$_n$(acac)$_{3-n}$] (n = 1, 2), the additional sharp peak (region C, 1320 cm^{-1}) appeared in the VCD spectra. Thus the peak was assigned to the C−O stretches intrinsic to tfac ligands with no ambiguity.

As another aspect, there were very broad absorption bands observed in the wavenumber region above 1650 cm^{-1} for some of the investigated complexes (e.g., Figure 2 (a) and (b) and Figure 3 (a)∼(d)). In those cases, the antipodes showed the absorption with opposite signs, excluding the possibility of baseline displacement. One possibility for these broad bands lies in the presence of the low-lying excited states particular to paramagnetic molecules.[19] In this respect, the present data may be a benchmark for the development of the theoretical approaches for open-shell molecules.

Experimental

Materials. Tris(acetylacetonato)ruthenium(III) ([Ru(acac)$_3$]) and (−)- or (+)-3-(trifluoroacetyl)camphor (denoted by (−)-tfacH or (+)-tfacH, respectively) (Aldrich) were used as purchased.

Syntheses and Purification of [Ru((−)- or (+)-tfac)(acac)$_2$]. A mixture of a free ligand ((−)-tfacH or (+)-tfacH) (0.40 g; 0.02 mol) and [Ru(acac)$_3$] (0.70 g; 0.02 mol) was kept in an autoclave for 16 h at 180 °C. The product was eluted on a silica gel column (30 mm (i.d.) × 600 mm) with benzene. Three bands were separated leaving unreacted [Ru(acac)$_3$] at the top of the column. From the mass spectral analyses, the first three bands were assigned to [Ru((−)-tfac)$_3$] (m^+/z = obs. 843; calc. 842.8), [Ru((−)-tfac)$_2$(acac)] (obs. 695; calc. 694.65) and [Ru((−)-tfac)(acac)$_2$] (obs. 547; calc. 546.52) in this order. The elemental analyses of these fractions were as follows: [Ru((−)-tfac)(acac)$_2$] (calcd) C, 51.32%; H, 5.49%; (found) C, 50.14% H, 5.08%; [Ru((−)-tfac)$_2$(acac)](calcd) C, 48.55%; H, 5.34%; (found) C, 48.35%, H, 5.16%; [Ru((−)-tfac)$_3$] (calcd) C, 51.31%; H, 5.29%; (found) C, 51.31%; H, 5.02%.

Separation of Diastereomeric Isomers. The separation of diastereomeric isomers of [Ru((−)-tfac)$_n$(acac)$_{3-n}$] (n = 1∼3) was performed by high performance liquid chromatography on a chiral column (4 mm (i.d.) × 25 cm) packed with an ion-exchange adduct of Δ-[Ru(phen)$_3$]$^{2+}$ (phen = 1,10-phenanthroline) and synthetic hectorite (Ceramosphere RU-1, Shiseido, Japan).[30] Each fraction containing ca. 10^{-4} mole of [Ru((−)-tfac)$_n$(acac)$_{3-n}$] (n = 1∼3) was eluted with methanol at 40 °C.The obtained chromatograms are shown in the Supporting Information (Figure S1). The details on the isomeric distribution among tris(tfac) complexes were described in the Supporting Information.[31] The electronic circular dichroism (ECD) spectra of the collected fractions are shown in the Supporting Information (Figures S2−S4). The Δ,Λ determination was made by comparing the CD spectra with those of Δ- and Λ-[Ru(acac)$_3$]. The separation of [Ru((+)-tfac)$_n$(acac)$_{3-n}$] (n = 1∼3) was performed in the same way on a column packed with Λ-[Ru(phen)$_3$]$^{2+}$/synthetic hectorite instead of Δ-[Ru(phen)$_3$]$^{2+}$/synthetic hectorite. The spectroscopic properties are given in Supporting Information Table S2 in the case of [Ru((−)-tfac)$_n$(acac)$_{3-n}$] (n = 1∼3) (the data for [Ru((+)-tfac)$_n$(acac)$_{3-n}$] (n = 1∼3) not shown).

X-ray Crystallographic Analyses. Single crystals of *trans*(I)-Λ-[Ru((−)-tfac)$_2$(acac)] were prepared by placing an open glass tube containing a methanol solution under water atmosphere. Single crystals appeared on the wall of the glass tube. A red needle-shaped crystal with dimension of 0.2 × 0.1 × 0.05 mm^3 was mounted on

a four-circle diffractometer (Mac Science M03XHF). Intensity data were collected with graphite-monochromatized Mo Kα radiation ($\lambda = 0.71073$ Å) by ω-2θ scan technique up to $2\theta = 50.0$ ° at 298 K. The intensities were corrected for Lorenz and polarization, and no absorption correction was applied. 2996 unique reflections were used for structure determination. The crystal data were $C_{29}H_{35}F_6O_6Ru$, monoclinic, *I*2, $a = 19.280(8)$ Å, $b = 8.913(4)$ Å, $c = 20.210(9)$ Å, $\beta = 105.75(3)°$, $Z = 4$, $D_x = 1.380$ Mg m^{-3}, $\mu = 0.538$ mm^{-1}. The structure was solved by direct method with SIR92[32a] and refined by full-matrix least-squares techniques with anisotropic thermal parameters for Ru, C, and O atoms using SHELXL97.[32b] The hydrogen atoms were located at the calculated positions. The trifluoromethyl groups were disordered between two orientations, and the fluorine atoms were refined with isotropic thermal parameters and occupancy factors of 0.5. The final *R* and R_w values were 0.115 and 0.257, respectively, and the *S* value was 1.176. The Flack factor for absolute structure was −0.06 (12).

Spectroscopic Measurements. NMR spectra were measured with a JNM-AL400 (JEOL, Ltd.) in $CDCl_3$. FAB-MS measurements were carried out with a JMS-700P, a JMS-HX110 or a JMS-700TZ (JEOL, Ltd.) for the identification of the synthesized compounds. UV−vis spectra were recorded with a U-2810 spectrophotomer (Hitachi, Ltd.). Circular dichroism (CD) spectra were recorded with a J-720 spectropolarimeter (JASCO, Co.). VCD and IR spectra were measured with a PRESTO-S-2007 spectrometer (JASCO, Co.). The special machine was developed for VCD measurements, being implemented with the shuttle system. A $CDCl_3$ solution of a complex (ca.0.01∼0.03 M) was injected into a cell (150 μm in optical length) with BaF_2 windows. The signal was accumulated during 1000 scans (ca. 10 min) for each complex. The VCD spectra of ligands were measured and accumulated 5000 scans, using a 50 μm cell by the shuttle system, in which the solvent effects were corrected at each 500 accumulation. The resolution was 4 cm^{-1}. The absorbance of IR spectra was adjusted below 1.0 for the optimal measurements.

Calculation Details. The IR and VCD spectra of these complexes were theoretically calculated by the use of *Gaussian 03* program.[33] VCD intensities were determined by the vibrational rotational strength and magnetic dipole moments, which were calculated by the magnetic field perturbation (MFP) theory formulated using magnetic field gauge-invariant atomic orbitals.[2] The MFP theory was implemented into *Gaussian 03* program.[33] Geometry optimization was performed at the DFT level (B3LYP functional with LANL2DZ for Ru(III) and 6-31G(d) for other atoms). The electronic configuration of Ru(III) ($(t_{2g})^5$) was specified as doublet in the open-shell system. Two types of *trans*-[Ru((+)-tfac)$_2$ (acac)] were assumed to belong to C_2 symmetry. Others were assumed to belong to C_1 symmetry. In the preliminary calculations, DFT calculation was performed for enantiomeric mono(tfac) complexes (Δ-[Ru((+)- or (−)-tfac)(acac)$_2$]), bis(tfac) complexes (*trans*(I)- Δ-[Ru((+)-tfac)$_2$(acac)], *trans*(II)- Δ-[Ru((+)-tfac)$_2$(acac)] and *cis*- Δ-[Ru((+)-tfac)$_2$(acac)]), and tris(tfac) complexes (*fac*-Δ-[Ru((+)-tfac)$_3$] and *mer*-Δ-[Ru((+)-tfac)$_3$]). In these calculations, trifluoromethyl groups were replaced by methyl groups. The vibrational frequencies and intensities were calculated after the geometry optimization. The optimization was performed using tight convergence, avoiding the numerical errors. No correction of introducing a scale factor was made. All of the calculation results were given in Supporting Information Figures S8−S10.

In order to improve the accuracy of the calculation results, further DFT calculation was made for mono(tfac) complex (Δ-[Ru((+)-tfac)(acac)$_2$]), bis(tfac) complex (*trans*(I)- Δ-[Ru((+)-tfac)$_2$(acac)]), and *fac*-Δ-[Ru((−)-tfac)$_3$] using the same basis set as before. In these calculations, no replacement of the CF_3 group in tfac was made with CH_3 group. As shown in the calculation results given in Supporting Information Figure S7 and Figure 5), more satisfactory agreement was obtained for the IR spectra of the molecule. Thus the peaks in the observed spectrum were assigned on the basis of the animations of molecular vibration with Gauss view 3.09 (Gaussian Inc.).

Conclusion

This study reports the first comprehensive VCD data for all members of mixed ligand complexes, Δ- or Λ-[Ru((−)-tfac)$_n$(acac)$_{3-n}$] or [Ru((+)-tfac)$_n$(acac)$_{3-n}$] ($n = 0$∼3), in the wavenumber region of 1000∼1800 cm^{-1}. By comparing the spectra among these molecules, the effects of ligand substitution, ΔΛ configuration, ligand chirality, and geometrical isomerism were discussed. As another aspect, some parts of the spectral features (e.g., C—O stretches) were predicted well by the VCD theory based on the magnetic field perturbation (MFP) in spite of the open-shell molecules.

Acknowledgment. We appreciate Prof. Toshihiro Kogure (The University of Tokyo) for the comments of VCD measurements, Ms. Keiko Nakata for her synthetic works, and Prof. Haruyuki Nakano (Kyusyu University) for the support of theoretical parts.

Supporting Information Available: The results of chromatographic resolution of [Ru((−)-tfac)$_n$(acac)$_{3-n}$], the ^{1}H NMR data of the diastereomeric isomers of [Ru((−)-tfac)$_n$(acac)$_{3-n}$], the values of ϵ and $\Delta\epsilon$, the circular dichorism spectra of Δ- or Λ-[Ru((−)-tfac)$_n$(acac)$_{3-n}$], the selected bond distances and angles from X-ray analyses, the VCD and IR spectra of (−) and (+)-tfacH ligand, [Ru(acac)$_3$], DFT calculated of VCD and IR of Δ-[Ru((+)-tfac)(acac)$_2$] and *trans*(I)- Δ-[Ru((+)-tfac)$_2$(acac)]. The results of DFT-calculated VCD and IR for Δ-[Ru((+)-tfac)(acac)$_2$], Δ-[Ru((−)tfac)(acac)$_2$], *trans*(I)-, *cis*- and *trans*(II)-Δ-[Ru((+)-tfac)$_2$(acac)] and *mer*- and *fac*-Δ-[Ru((+)-tfac)$_3$]. These calculations were made for the simplified model that trifluoromethyl groups were replaced by methyl groups. This material is available free of charge via the Internet at http://pubs.acs.org.

IC801971P

(33) Fisch, M. J.; Trucks, G. W.; Schlegel, H. B.; Scuseria, G. E.; Robb, M. A.; Cheeseman, J. R.; Montgomery, J. A.; Vreven, Jr. T.; Kudin, K. N.; Burant, J. C.; Millam, J. M.; Iyengar, S. S.; Tomasi, J.; Barone, V.; Mennucci, B.; Cossi, M.; Scalmani, G.; Rega, N.; Petersson, G. A.; Nakatsuji, H.; Hada, M.; Ehara, M.; Toyota, K.; Fukuda, R.; Hasegawa, J.; Ishida, M.; Nakajima, T.; Honda, Y.; Kitao, O.; Nakai, H.; Klene, M.; Li, X.; Knox, J. E.; Hratchian, H. P.; Cross, J. B.; Adamo, C.; Jaramillo, J.; Gomperts, R.; Stratmann, R. E.; Yazyev, O.; Austin, A. J.; Cammi, R.; Pomelli, C.; Ochterski, J. W.; Ayala, P. Y.; Morokuma, K.; Voth, G. A.; Salvador, P.; Dannenberg, J. J.; Zakrzewski, V. G.; Dapprich, S.; Daniels, A. D.; Strain, M. C.; Farkas, O.; Malick, D. K.; Rabuck, A. D.; Raghavachari, K.; Foresman, J. B.; Ortiz, J. V.; Cui, Q.; Baboul, A. G.; Clifford, S.; Cioslowski, J.; Stefanov, B. B.; Liu, G.; Liashenko, A.; Piskorz, P.; Komaromi, I.; Martin, R. L.; Fox, D. J.; Keith, T.; Al-Laham, M. A.; Peng, C. Y.; Nanayakkara, A.; Challacombe, M.; Gill, P. M. W.; Johnson, B.; Chen, W.; Wong, M. W.; Gonzalez, C.; Pople, J. A. *Gaussian 03, Revision C. 02*; Gaussian, Inc., Wallingford, CT, 2004.